Available online at www.sciencedirect.com

SciVerse ScienceDirect

Ceramics International 38 (2012) 2483–2493

CERAMICS INTERNATIONAL

www.elsevier.com/locate/ceramint

Interaction between low-grade magnesium oxide and boric acid in chemically bonded phosphate ceramics formulation

J. Formosa [a,b,*], J.M. Chimenos [a], A.M. Lacasta [c], M. Niubó [a,c]

[a] Departament de Ciència dels Materials i Enginyeria Metal·lúrgica, Universitat de Barcelona, Martí i Franquès 1, 08028 Barcelona, Spain
[b] Departament de Construccions Arquitectòniques II, Universitat Politècnica de Catalunya, Av. Dr. Marañón 44-50, 08028 Barcelona, Spain
[c] Departament de Física Aplicada, Universitat Politècnica de Catalunya, Av. Dr. Marañón 44-50, 08028 Barcelona, Spain

Received 10 October 2011; received in revised form 4 November 2011; accepted 5 November 2011
Available online 11 November 2011

Abstract

A hard-burner low-grade MgO (LG-MgO) is used to formulate a chemically bonded phosphate ceramic (CBPC) instead of pure MgO. This by-product is 10 times cheaper than pure MgO. The use of this by-product reduces the cost of the final material and therefore an economical construction material could be obtained. This would reinforce the criteria of sustainability and recyclability. In addition, the inert phases contained on LG-MgO act like inorganic fillers, improving the mechanical properties of this CPBC, which can be considered as a mortar. A range from 55% to 65% of LG-MgO is studied, and boric acid is added in order to improve workability and setting times. Design of Experiments (DoEs) approach enabled the evaluation of the influence of each component and the interactions between them. According to the setting times and compressive strength results, a formulation range is proposed.

Keywords: C. Mechanical properties; D. MgO; E. Structural applications; Design of Experiments; Recycling

1. Introduction

Portland cement is the most widely used hydraulic cement in the world, because it covers a wide range of properties and possibilities and is an inexpensive material. However, in recent years other more specific types of cements have been developed, which are able to extend the range of work and their applications in other fields of technology. These types of newly developed cements include those known as chemically bonded ceramics (CBCs) [1]. CBCs are ceramic materials possessing certain characteristics of cement and thus can be considered as such. In general, CBCs are obtained from the acid–base chemical reaction into an aqueous phase between a metal cation and an oxoanion source. When phosphates are used as oxoanion raw material, the CBC becomes chemically bonded phosphate ceramic (CBPC). These CBPCs are frequently used as stabilizing agents [2] and/or for the encapsulation of hazardous substances with a high potential for leaching [3–5] radioactive substance [6]. Moreover, CBPC presents very fast setting time and good mechanical properties; for this reason CBPCs can also be used as materials for the quick repair of concrete structures [7,8].

The phosphate binders are formed by an acid–base aqueous reaction between a divalent or trivalent oxide and an acid phosphate or phosphoric acid. In this reaction the metal oxide dissolves and reacts with the phosphate ions to form a phosphate gel as a precursor of the solid structure. The reaction slurry hardens rapidly at room temperature. It is possible to use different phosphates and metal oxides sources for the formation of cold-setting ceramics, e.g. potassium or ammonium phosphates and iron, magnesium, aluminium, zinc or calcium oxides. During the chemical curing process, the steps controlling the formation of CBPC are the dissolution and hydrolysis of metal oxides. However, the setting rates can be controlled by a suitable selection of oxides [9]. It is known that the solubility of divalent metal oxides in acidic or neutral pHs is higher than trivalent metal oxides. Furthermore, the solubility needed to form CBPC is between these two metal oxides [10].

* Corresponding author at: Departament de Ciència dels Materials i Enginyeria Metallúrgica, Universitat de Barcelona, Martí i Franquès 1, 08028 Barcelona, Spain. Tel.: +34 934 037244; fax: +34 934 035438.
E-mail address: joanformosa@ub.edu (J. Formosa).

0272-8842/$36.00
doi:10.1016/j.ceramint.2011.11.017

Nomenclature

LG-MgO	low-grade MgO
CBPCs	chemically bonded phosphate ceramics
CBPC	chemically bonded phosphate ceramic
DoE	Design of Experiment
CBCs	chemically bonded ceramics
CBC	chemically bonded ceramic
MKP	mono potassium phosphate
HB	boric acid
LG	LG-MgO
IST	initial setting time
FST	final setting time
CS	compressive strength
HB/S	boric acid to solid ratio
F1	optimum formulation suggested number 1
F2	optimum formulation suggested number 2
F2	optimum formulation suggested number 3

It is thus reported in the literature that the aqueous reaction of magnesium oxide (MgO) with monopotassium phosphate (KH_2PO_4; MKP) results in the crystalline structure of K-struvite ($KMgPO_4{\cdot}6H_2O$), which behaves as concrete and is frequently known as ceramicrete [10,11].

The use of highly reactive magnesium oxides, such as pure caustic MgO, results in very strong reactions that lead to the formation of precipitates without forming monolithic ceramics [9], and also decreases mechanical properties of these materials. However, the setting time of the magnesium CBPC may be improved by reducing the dissolution rate of MgO by a prior calcination of this raw material [2,10,12].

The main drawback of K-struvite formation for possible use as solid waste cement or for repairing concrete structures is the high cost of raw materials, not to mention the costs arising from the calcination process for appropriate treatment of the MgO. These aspects have been widely studied and cited in the literature, and from the economic point of view it is considered preferable to use setting retardants such as boric acid (H_3BO_3, HB) rather than pre-calcined MgO [13,14]. The economic factor should therefore be taken into consideration when using this CBPC.

Nevertheless, it is possible to use less expensive sources of magnesium oxide; for example, the use of low-grade MgO (LG-MgO) as raw material could be a feasible alternative because LG-MgO is 10 times cheaper than pure MgO. LG-MgO, an industrial by-product obtained during the calcination of natural magnesia, has been used by the same authors with very promising results for the removal and recovery of phosphates and ammonium contained in high strength wastewater [15,16]. In these case studies the presence of struvite ($NH_4MgPO_4{\cdot}6H_2O$) and newberyite ($MgHPO_4{\cdot}3H_2O$) were respectively identified in the precipitates obtained. Moreover, the use of an industrial by-product may reduce the cost of the final product and provide a competitive alternative to commonly used mortar cements, while reinforcing criteria of sustainability and recyclability.

The use of a heavily calcined magnesia by-product (≈1200 °C) considerably reduces MgO reactivity and solubility and increases the setting time of the CBPC. At the same time, costs arising from magnesia calcination are avoided. An earlier study carried out by the authors showed that the use of LG-MgO to obtain CBPC is feasible [17]. Very promising results were obtained, but an exhaustive study of some parameters controlling the acid–base reaction is necessary in order to improve the setting time, workability and physico-chemical properties. The accomplished objectives enable the use of the CBPC formulated with LG-MgO as a cheap material for repairing concrete structures or encapsulating hazardous waste, for example.

Several studies included the use of Design of Experiments (DoEs) in order to optimize the experimental procedure [18,19]. The main goal of the present paper is to evaluate the effect of LG-MgO and HB on the composite properties. The implementation of a factorial design model using Design of Experiments (DoEs) made possible to extract the maximum information of the experiments performed. Both factors were chosen (LG-MgO and HB) and their effects on the composite properties were quantified. Predictive theoretical mathematical models were determined for each response, allowing to estimate the composites behaviour as well as to find the adequate formulation from required properties.

2. Experimental procedure

The experimental procedure described below began with preliminary studies carried out by the authors [17]. Taking into account the MgO content and the low reactivity of the LG-MgO used in the CBPC formulation, a water to solid ratio (W/S) and a weight proportion range of MKP and LG-MgO were established. Although the results obtained were promising, and proved to be even better than those using pure MgO [11], the mixtures formulated with LG-MgO still showed short setting times and poor workability. In accordance with these results, in the present work, the addition of HB in order to extend the setting time and improve workability has been studied and evaluated using DoE.

2.1. Design of Experiments

Usually the effect of mineral filler addition on the blend has been analyzed individually, by a ‘‘trial and error’’ approach. The DoE technique helps to verify whether or not there is a synergistic effect between the variables on the final properties of the composite or parameters affecting its manufacturing [20,21]. The selected Design of Experiments was a response surface three level factorial plan for two variables. The experimental procedure was created and analyzed with the ‘‘Design Expert 7.0’’ software.

LG-MgO concentration (referred as LG in DoE mortar formulation) was varied from 55 to 65 wt% versus MKP. HB was added from 0 to 3 wt%, where HB percentage refers to the weight of the solid mixture of MKP and LG-MgO, and is considered as an extra addition to the mortar formulations. The

Table 1
CBPC compositions tested.

Reference	Solid (S)		HB/S (%)
	LG-MgO (%)	MKP (%)	
55LG	55	45	0.00
55LG0.25HB	55	45	0.25
55LG0.50HB	55	45	0.50
55LG0.75HB	55	45	0.75
55LG1HB	55	45	1.00
55LG2HB	55	45	2.00
55LG3HB	55	45	3.00
60LG	60	40	0.00
60LG0.25HB	60	40	0.25
60LG0.50HB	60	40	0.50
60LG0.75HB	60	40	0.75
60LG1HB	60	40	1.00
60LG2HB	60	40	2.00
60LG3HB	60	40	3.00
65LG	65	35	0.00
65LG0.25HB	65	35	0.25
65LG0.50HB	65	35	0.50
65LG0.75HB	65	35	0.75
65LG1HB	65	35	1.00
65LG2HB	65	35	2.00
65LG3HB	65	35	3.00

formulations tested are shown in Table 1. Performing of the different runs must be random to minimize systematic and/or cumulative errors on the final results and the analysis of DoE results is based in the analysis of variance (ANOVA) [20]. In this case, p and F values have been used to interpret the obtained results. The p-value indicates whether the factor has a significant contribution to the model, represents the smallest level of significance that would lead to rejection of the null-hypothesis (i.e. there is no effect of the controllable factor on the response under investigation) while this hypothesis is true. A p-value lower than the level of significance ($\alpha = 0.05$) indicates significant contribution of the factor with a 95% of confidence. In other words, if a p-value in a test for the significance of a certain factor is smaller than 0.05, this factor is considered statistically significant at $\alpha = 0.05$ level of significance. The F value is defined as the ratio of the Model SS/Residual SS, where Model SS and residual SS are referred to the regression and error sum of squares respectively. Large F values indicate significant contribution while small values denote that the variance could be affected by noise.

2.2. Materials

The low-grade magnesium oxide (LG-MgO) is supplied by Magnesitas Navarras S.A. based in Navarra (Spain). This LG-MgO is derived from the calcination of natural magnesite in rotary kiln at 1100 °C. It is a by-product collected as cyclone dust in the fabric filters from the air pollution control system. Around 100 kg of LG-MgO was taken from various stockpiles. The sample was previously homogenized, quartered to a 1/16 split and dried in an oven at 105 °C for 24 h in order to obtain a representative sub-sample of about 500 g for physical and chemical characterization.

The source of phosphate employed for this study is mono potassium phosphate (MKP), KH_2PO_4, food grade, which is commonly used as a fertilizer. A boric acid, Optibor® technical grade (HB), H_3BO_3, supplied by Borax España, S.A. (Castellón, Spain), was also used as a setting time retardant.

2.3. LG-MgO physico-chemical characterization

LG-MgO was analyzed by X-ray fluorescence (XRF) using a Philips PW2400 X-ray sequential spectrophotometer to elucidate major and minor elements. X-ray diffraction (XRD) was performed in a Bragg–Brentano Siemens D-500 powder diffractometer with Cu Kα radiation in order to determine the crystalline phases. Particle size distribution was obtained with a laser analyser Beckman Coulter LS 13 320. Density was measured with a helium pycnometer and the specific surface area by the BET single point method with a Micromeritics porosimeter.

To quantify the carbonate phases contained in the LG-MgO, a thermogravimetric analysis (TGA) was employed to evaluate the thermal decomposition in nitrogen atmosphere (100 mL min^{-1}) up to 1000 °C using a TA Instruments SDT Q600 Simultaneous TGA-DSC. It should be noted that the MgO contained in carbonated phases is not available to form CBPC and should not be taken into account to determine the MgO/MKP weight ratio.

Finally, a citric acid test was performed in order to evaluate MgO reactivity. The citric acid activity test is designed for determining the reactivity of MgO by acid neutralization using phenolphthalein as indicator. The magnesia activity time is the time elapsed between the addition of acid and the formation of a reddish colour [22]. Acid neutralization values of less than 60 s are used to define highly reactive (soft-burnt) MgO. Medium reactive MgO gives a measurement between 180 and 300 s, while a low reactivity MgO (hard-burnt) gives a value of greater than 600 s and a dead-burnt MgO value greater than 900 s [23].

2.4. Chemically bonded phosphate cements formulation and preparation

An earlier study [17] showed that, as a consequence of the low grade, reactivity and particle size distribution of the magnesia by-product (see Section 3.1), the LG-MgO/MKP weight ratio should be roughly that of the reversed ratio described in the literature for pure MgO (23/77). For these LG-MgO/MKP formulations, a water to solid (W/S) ratio of 0.24 showed the normal consistency determined by the standard EN 196-3. It is known that the excess of water is not chemically bound within the hardened cement, leaving a porous structure during curing period, and, consequently, poor mechanical properties [24].

Thus, in all the experimental series in the present research work, the W/S ratio was fixed at 0.24. Accordingly, the CBPC was prepared as a mixture of the different solid reagents in weight and then the kneading water was added. All mixtures were stirred with a hand-drill for 4 min. Formulations with different amounts of LG-MgO and MKP around the weight

ratio (60/40) were considered in order to determine an optimum proportion. Likewise, different amounts of HB were added in order to extend the setting time and improve workability. In all cases, initial and final setting times and soundness were measured by the Vicat method (EN 196-3). The composition of the different mixtures, as is commented above, is summarized in Table 1.

The resulting CBPC wet formulation was cast in prismatic moulds with dimensions of 40 mm × 40 mm × 160 mm to perform mechanical properties. Specimens were left in their moulds for 24 h in a curing chamber at a constant temperature of 20 ± 2 °C and a relative humidity of 95%, and the unmolded mortars were further allowed to cure in the same conditions up to different ages (1, 7 and 28 days, respectively).

2.5. Testing procedures

For all formulations the initial and final setting time of the mixtures were measured with a manual Vicat needle apparatus, following the standard EN 196-3. The three-point flexural tensile strength and the compressive strength tests were performed in a mechanical testing machine Incotecnic MUTC-200, at a loading rate of 5 kg s^{-1} according to standard EN 196-1. In order to study the effect of the curing time on the mechanical properties, three different curing times (1, 7 and 28 days) were considered. Before testing mechanical properties, specimens were left in the oven for 4 h at 60 °C and then 2 h at room temperature.

2.6. Cement structure characterization

Some specimens showing good mechanical results and workability were characterized to determine the structure of the material formed. Thus, XRD patterns were obtained to determine the crystalline phases and the occurrence of chemically bonded magnesium phosphates. Likewise, the cement microstructure of the same formulations was studied by SEM-EDS backscattering mode (EBSD) using a Leica Cambridge Stereoscan S360. Semi-quantitative X-ray analyses were performed in order to determine both the most interesting elements in a specimen and a rough measure of their abundance, especially as trends across a sample. The X-ray maps were generated using the abundance of an element as the intensity of the image, showing the distribution of the specified elements. Moreover, line-scan profiles were also collected, which enabled the abundance of an element with distance along a specified line to be plotted. This is especially helpful for examining concentration gradients within a sample.

3. Results and discussion

3.1. LG-MgO characterization

Characterization of the LG-MgO was carried out by means of the different techniques described in Section 2.3. The chemical composition obtained from XRF is given in Table 2 for each determined element as the most stable corresponding oxide. As expected, magnesium turns out to be the main element content in LG-MgO. The presence of calcium and silica should also be noted. The diffraction pattern of the magnesium by-product (Fig. 1) shows periclase –MgO– as the major phase and unburned magnesite –$MgCO_3$– as a minor one, as well as dolomite –$MgCO_3{\cdot}CaCO_3$–, quartz –SiO_2– and calcite (or aragonite) –$CaCO_3$–, which occurs in natural magnesite, and lime –CaO– and anhydrite –$CaSO_4$– generated during the calcination of dolomite [25].

Table 2
Physicochemical characterization of LG-MgO.

	LG-MgO (%)
MgO	63.66
CaO	9.91
SiO_2	2.04
Fe_2O_3	2.42
SO_3	4.10
Al_2O_3	0.22
K_2O	0.27
V_2O_5	0.15
MnO	0.13
Loss of ignition (LOI)	16.96
Density (g cm^{-3})	3.2
Specific surface (m^2 g^{-1})	10.4

LOI: loss of ignition (1100 °C).

Fig. 2 shows the thermal decomposition up to 1000 °C of LG-MgO in nitrogen atmosphere. The TG curve shows a total mass loss of about 17.0%, which is very close to the LOI determined by XRF (see Table 2). This total mass loss takes place in five consecutive stages [25]. The mass loss below 200 °C corresponds to the release of the moisture content and water absorbed into the pores of the LG-MgO. The second stage corresponds to the thermal dehydroxylation of $Mg(OH)_2$. The mass loss in the range of 450–625 °C is due to the decarbonation of $MgCO_3$. The fourth stage in the range of 625–757 °C is attributed to the thermal decomposition of $MgCO_3{\cdot}CaCO_3$. The last stage in the range of 757–975 °C is due to decarbonation of $CaCO_3$ contained in the LG-MgO.

According to the mass loss attributed to the decarbonation of $MgCO_3$ and $MgCO_3{\cdot}CaCO_3$, it is possible to determine the content of MgO in these carbonated phases (4.61% and 1.55%, respectively). Hence, taking into account the total percentage of

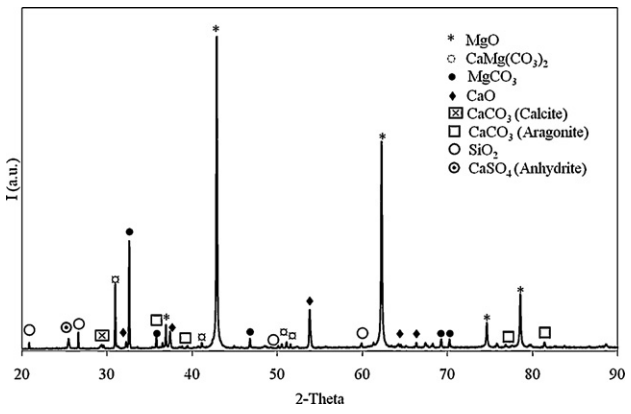

Fig. 1. X-ray pattern of LG-MgO.

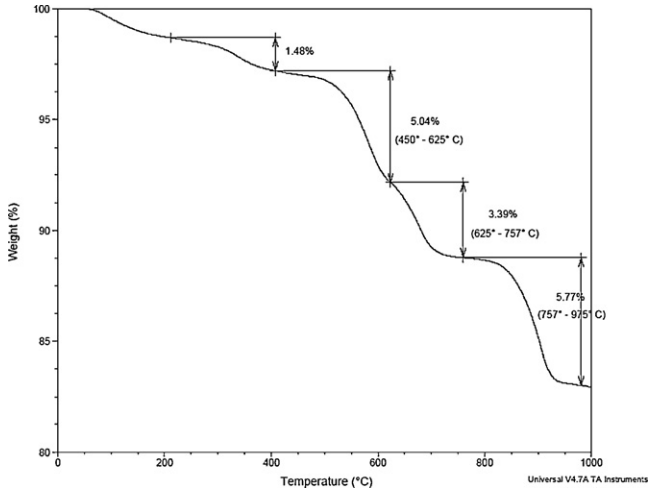

Fig. 2. TG curves of LG-MgO thermal decomposition up to 1000 °C in nitrogen atmosphere.

MgO determined by XRF (see Table 2) and the content of this MgO in the carbonated phases, the MgO available to form the CBPC formulated with LG-MgO is approximately 57.50%.

A low specific BET surface area value (see Table 2) compared with commercial pure caustic magnesia [9,12] should be noted. This fact may be explained by the greater sintering degree that takes place during the calcination process of natural magnesite. By increasing the temperature or calcination time, the crystalline imperfections decrease, and as a consequence so does the activity of the magnesia.

The low specific surface area of the LG-MgO agrees with the high value obtained in the citric acid activity test, whose results were greater than 780 ± 35 s. According to these values, the LG-MgO tested should be termed ''hard-burned'' magnesia. However, it should be noted that the content of CaO in the LG-MgO is about 2.57% (determined from the total CaO content and the TG analysis), which is also involved in the neutralization of acid and shows a higher reactivity than MgO.

Particle size distributions are given in Table 3, expressed as the accumulative fraction smaller than the particle size (d_x). Table 3 also shows the particle size distribution of MKP. The particle size distribution is an important parameter in the mortar industry due to its influence on the mechanical properties and rate of dissolution of these reagents. As may be observed, the particle size of MKP is greater than LG-MgO used in the formulation of CBPC. However, it should be taken into account that whereas MKP is a water soluble phase, LG-MgO shows lower reactivity and remains roughly insoluble (see below).

Table 3
Particle size distributions.

Parameter (μm)	LG-MgO	MKP
d_{90}	106	707
d_{50}	34	331
d_{10}	2	163

3.2. CBPC. Physical and mechanical characterization

In every case the models obtained were statistically significant with large F values (14.38 for initial setting time and 22.30 for final setting time) and small probabilities of them being originated by noise. Statistical analysis of initial and final setting time values reveals that the factors under investigation (LG and HB) had a significant influence as main effects on this response. Mortar samples were prepared as described in Section 2.4, according to the formulations given in Table 1, and Table 4 shows the results obtained for the formulations tested. However, taking into account the MgO content available in the LG-MgO (see Section 3.1), the molar ratio MgO/MKP ranged from 1.9 to 4.5, which is approximately 1.3–3.1 times greater than the molar ratio described in the bibliography for CBPC formulated with pure MgO [11]. However, the cement paste formulated using 50% of LG-MgO (50LG) gave rise to the formation of precipitates without forming a homogeneous paste. Therefore 50LG dosages were discarded in the present study. Dosages with a 70% of LG-MgO were also carried out and subsequently discarded due to a depletion of the mechanical properties. See Table 5 where the standard analysis of variance (ANOVA) was performed for initial and final setting time.

Figs. 3 and 4 show the initial and final setting time values surface plot. As mentioned above, to enhance the implementation of the CBPC it is necessary improve the setting time in order to increase the workability of this material. It is therefore important that the initial setting time be as high as possible, and in fact the final setting time differed very little from this. As can be observed in these figures, an increase of LG leads in a diminution of the initial setting time (p-value = 0.0024) and final setting time (p-value = 0.002), this effect is due to the acceleration of the acid–base, therefore the mortars set faster. An increase in HB percentage leads to an increase both the initial (p-value < 0.0001) and the final setting times (p-value < 0.0001). If both LG and HB are increased together the

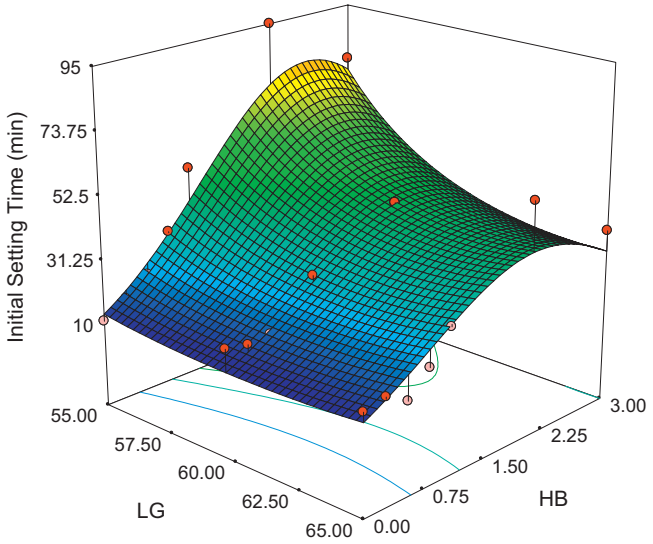

Fig. 3. Surface plot of the initial setting time as a function of LG and HB.

Table 4
Experimental results of the formulations tested.

Reference	Initial setting time (min)	Final setting time (min)	CS 1 day (MPa)	CS 7 days (MPa)	CS 28 days (MPa)
55LG	11.00 ± 2.00	20.00 ± 2.00	36.29 ± 1.99	33.01 ± 3.38	23.67 ± 1.45
55LG0.25HB	16.00 ± 2.00	31.50 ± 2.00	31.60 ± 2.40	29.42 ± 3.20	27.43 ± 5.02
55LG0.50HB	21.75 ± 2.00	52.75 ± 2.00	24.23 ± 5.04	27.75 ± 2.41	25.56 ± 5.42
55LG0.75HB	34.00 ± 2.00	75.00 ± 2.00	29.01 ± 0.83	30.14 ± 2.10	25.26 ± 3.26
55LG1HB	53.50 ± 2.00	109.00 ± 2.00	7.97 ± 0.85	23.77 ± 2.27	26.79 ± 2.49
55LG2HB	95.00 ± 2.00	120.00 ± 2.00	1.10 ± 0.19	25.63 ± 2.62	27.06 ± 1.81
55LG3HB	76.00 ± 2.00	102.00 ± 2.00	1.08 ± 0.09	20.53 ± 1.25	24.10 ± 0.67
60LG	18.00 ± 2.00	32.00 ± 2.00	41.25 ± 3.56	39.86 ± 8.43	38.07 ± 4.41
60LG0.25HB	16.50 ± 2.00	32.00 ± 2.00	34.64 ± 3.49	40.72 ± 5.34	44.75 ± 3.59
60LG0.50HB	17.00 ± 2.00	34.00 ± 2.00	31.42 ± 4.20	32.96 ± 5.69	41.14 ± 3.31
60LG0.75HB	18.50 ± 2.00	35.50 ± 2.00	32.94 ± 3.50	35.25 ± 8.65	37.27 ± 1.80
60LG1HB	31.00 ± 2.00	65.50 ± 2.00	30.91 ± 1.90	28.22 ± 2.91	33.24 ± 1.31
60LG2HB	45.50 ± 2.00	81.00 ± 2.00	2.66 ± 0.23	37.63 ± 3.62	32.57 ± 5.44
60LG3HB	24.00 ± 2.00	60.00 ± 2.00	1.55 ± 0.10	27.92 ± 1.92	28.93 ± 2.05
65LG	15.50 ± 2.00	36.00 ± 2.00	32.08 ± 3.11	37.63 ± 3.62	38.01 ± 1.04
65LG0.25HB	17.00 ± 2.00	29.00 ± 2.00	35.04 ± 2.20	40.95 ± 2.83	51.09 ± 3.53
65LG0.50HB	12.50 ± 2.00	30.00 ± 2.00	27.26 ± 1.54	35.39 ± 3.90	41.61 ± 3.21
65LG0.75HB	20.00 ± 2.00	34.50 ± 2.00	41.46 ± 3.77	41.29 ± 2.65	52.95 ± 3.53
65LG1HB	30.00 ± 2.00	65.00 ± 2.00	25.25 ± 1.67	32.96 ± 1.98	40.07 ± 2.38
65LG2HB	59.50 ± 2.00	79.00 ± 2.00	2.77 ± 0.36	26.64 ± 1.02	27.65 ± 1.48
65LG3HB	40.00 ± 2.00	60.00 ± 2.00	1.62 ± 0.10	20.14 ± 1.62	21.19 ± 1.22

Table 5
ANOVA results for initial and final setting time.

Source	Degrees of freedom	Initial setting time			Final setting time		
		Sum of squares	Mean square	p-Value prob > F	Sum of squares	Mean square	p-Value prob > F
Model	5	8480.10	1696.02	<0.0001	16237.72	3247.54	<0.0001
LG	1	1446.57	1446.57	0.0024	2984.82	2984.82	0.0002
HB	1	5058.47	5058.47	<0.0001	8288.36	8288.36	<0.0001
LG-HB	1	681.80	681.80	0.0266	806.01	806.01	0.0296
LG^2	1	797.81	797.81	0.0176	760.91	760.91	0.0339
HB^2	1	1203.40	1203.40	0.0048	3717.16	3717.16	<0.0001
Residual	19	2240.99	117.95		2767.44	145.65	
Lack of fit	15	2240.99	149.40		2767.44	184.50	
Pure error	4	0.000	0.000		0.000	0.000	
Cor. total	24	10721.09			19005.16		

effect on the initial and final setting time response is found to be lower than that expected from the sum of each one separately. Hence, it can be concluded that there is a negative interaction between these two factors (p-value = 0.0266 for initial time and p-value = 0.0296 for final time). Boric acid forms a temporary coating of lunebergite –$Mg_3B_2(PO_4)_2(OH)_6{\cdot}6H_2O$– on the surface of oxide particles, which prevents the dissolution of magnesium oxide into the solution. As the oxide powder is mixed into the solution, the pH rises and the coating itself dissolves [24]. Thus, an improvement of workability was obtained when HB is added.

As can be observed in Figs. 3 and 4, the retarding setting time is higher when the LG/HB ratio is increased. Thus, for the addition of the same HB percentage, the increase in the setting time becomes more notable in a minor LG/HB ratio. The increase in the setting time takes place up to a maximum addition of about 2.0% of HB, and thereafter the setting time remains practically constant. An initial setting time greater than 20 min is assumed as a good workability. This behaviour is achieved with additions greater than 0.5% of HB in the mortar formulations.

All the results derived from the modification of any of the controllable variables can be translated into a predictive mathematical model. For the initial and final setting time results, the model can be written according to the following equations, corresponding to the mathematical models for initial setting time values (IST), and final setting time values (FST) respectively:

$$\mathrm{IST} = 1697.28 - 56.57\mathrm{LG} + 125.98\mathrm{HB} - 1.41\mathrm{LG}\cdot\mathrm{HB} + 0.47\mathrm{LG}^2 - 8.76\mathrm{HB}^2 \quad (1)$$

$$\mathrm{FST} = 1717.59 - 55.99\mathrm{LG} + 157.47\mathrm{HB} - 1.53\mathrm{LG}\cdot\mathrm{HB} + 0.46\mathrm{LG}^2 - 15.38\mathrm{HB}^2 \quad (2)$$

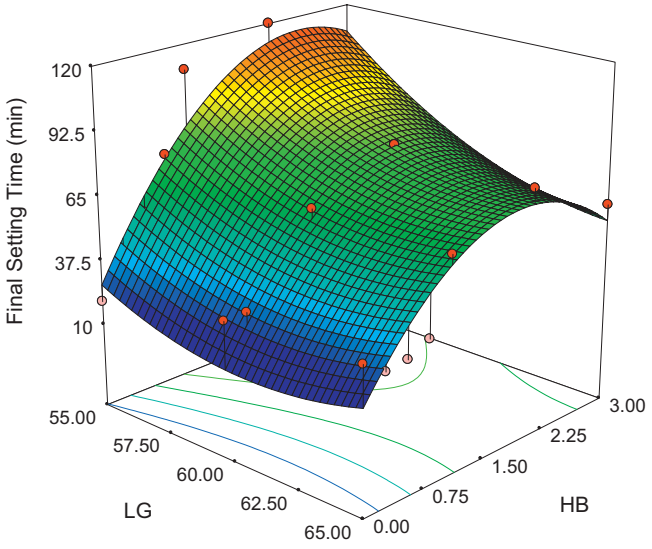

Fig. 4. Surface plot of the final setting time as a function of LG and HB.

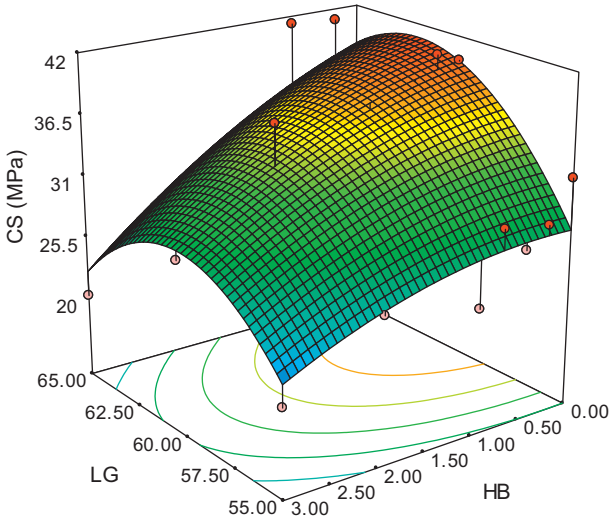

Fig. 6. Surface plot of the compressive strength at 7 days as a function of LG and HB.

This model can quantitatively predict the response within the operating range of controllable variables. It can also give some suitable formulations when a certain response is required. The model only incorporates the factors and interactions considered statistically significant. In both cases a surface quadratic model describes the system.

Figs. 5–7 show the mechanical compressive strength (CS) of the CBPC specimens after being cured for 1, 7 and 28 days, respectively. The ANOVA results were performed for each parameter and are summarized in Table 6. Statistical analysis of CS values at 1 day (Model F value = 96.38) reveals that the factor under investigation HB had a significant influence as main effects on this response (p-value < 0.0001). There are no interactions between factors. As can be observed in all these figures, the comparison of formulations without HB showed a slight increase of CS when the percentage of LG is also increased at the same curing time. However, LG addition has no significance influence (p-value = 0.1052) in compressive values at 1 day as can be seen in Fig. 5. On the other hand, formulations with an HB/S ratio greater than 1.0% show the worst CS values, which is in accordance with that described in Ref. [9]. Thus, as can be seen in Fig. 5, the formulations with high amounts of HB showed weak CS when the curing time was 1 day. This fact is remarkable in the formulations with low content of LG, whose CS fell sharply with an increasing addition of HB. However, formulations with high content of LG showed a marked decrease in CS only when the addition of HB was higher than 1.0%. Accordingly, it is concluded that the addition of large amounts of HB requires more time to harden sufficiently.

Statistical analysis of CS values at 7 days (Model F value = 8.16) reveals that the factors under investigation LG

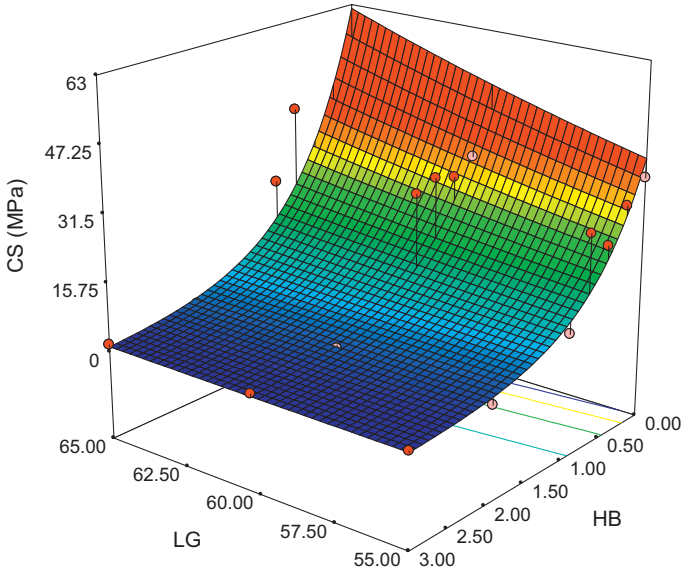

Fig. 5. Surface plot of the compressive strength at 1 day as a function of LG and HB.

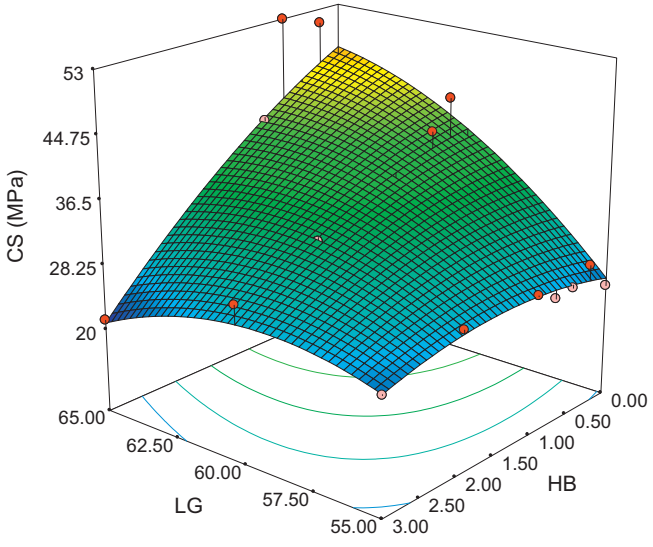

Fig. 7. Surface plot of the compressive strength at 28 days as a function of LG and HB.

Table 6
ANOVA results for CS at 1, 7 and 28 days.

Source	Degrees of freedom	CS at 1 day			Degrees of freedom	CS at 7 days			CS at 28 days		
		Sum of squares	Mean square	p-Value prob > F		Sum of squares	Mean square	p-Value prob > F	Sum of squares	Mean square	p-Value prob > F
Model	2	41.59	20.80	<0.0001	5	664.82	132.96	0.0003	1369.94	273.99	<0.0001
LG	1	0.62	0.62	0.1052	1	72.50	72.50	0.0484	268.96	268.96	0.0007
HB	1	40.98	40.98	<0.0001	1	304.65	304.65	0.0004	449.62	449.62	<0.0001
LG-HB					1	38.18	38.18	0.1423	253.27	253.27	0.0010
LG^2					1	232.16	232.16	0.0013	90.21	90.21	0.0314
HB^2					1	9.65	9.65	0.4509	18.15	18.15	0.3102
Residual	22	4.75	0.22		19	309.58	16.29		317.31	16.70	
Lack of fit	18	4.75	0.26		15	309.58	20.64		317.31	21.15	
Pure error	4	0.000	0.000		4	0.000	0.000		0.000	0.000	
Cor. total	24	46.34			24	974.40			1687.25		

(p-value = 0.0484) and HB (p-value = 0.0004) had a significant influence as main effects on this response. After 7 days of curing (Fig. 6), the samples containing large amounts of HB (i.e. HB/S ratios of 2.0–3.0%) did not show such a sharp decrease as in CS, although a slight decrease in the mechanical property was observed according to the amount of HB added. The best mechanical properties are obtained with low HB content and 60% of LG. For specimens formulated with 60% or 65% of LG, the CS did not show great differences between those pastes cured for 1 or 7 days, which are from 30 to 40 MPa. The same conclusion may be drawn for all specimens cured for 28 days (Fig. 7).

Statistical experimental results for the analysis of CS values at 28 (with Model F value = 16.41) days reveals that the factors under investigation LG and HB had a significant influence as main effects on this response (p-values = 0.0007 and <0.0001 respectively), in addition it is found an interaction between factors LG and HB (p-value = 0.001), when they are added together lower results of CS are obtained. Those results were very similar to those shown in Fig. 6. These CS values are higher than those described in the literature for CBPC formulated with pure caustic MgO calcined at high temperatures (Ceramicrete®, 23 MPa), and are within the range of results obtained for the magnesium CBPC formulated with inorganic fillers (e.g. fly ash, 15–83 MPa) [10,11].

In general, the specimens 60LG with different HB percentage present similar CS properties at 1 day and 7 days, and remain less affected when HB is increased. Likewise, in addition to the high CS, the experimental series formulated with 60% of LG showed a lower dispersion of values, and the profile of the curve shows a clear trend according to the addition of HB, which can be attributed to the greater homogeneity of the material.

The mathematical models for compressive strength values (at 1, 7 and 28 days) are shown in the following equations, respectively:

$$\mathrm{Ln}\ (\mathrm{CS}\ (1\,\mathrm{day})) = 1.40 + 0.04\mathrm{LG} - 1.32\mathrm{HB} \quad (3)$$

$$\mathrm{CS}\ (7\,\mathrm{days}) = -933.27 + 31.43\mathrm{LG} + 18.72\mathrm{HB} - 0.33\mathrm{LG}\cdot\mathrm{HB} - 0.25\mathrm{LG}^2 - 0.78\mathrm{HB}^2 \quad (4)$$

$$\mathrm{CS}\ (28\,\mathrm{days}) = -664.15 + 21.22\mathrm{LG} + 50.39\mathrm{HB} - 0.86\mathrm{LG}\cdot\mathrm{HB} - 0.15\mathrm{LG}^2 - 1.08\mathrm{HB}^2 \quad (5)$$

For equation corresponding to CS at 1 day a data transformation has been applied to improve the predictive model, a response surface linear model describes the overall system and in the rest of cases a surface quadratic model explains the system.

On the basis of the statistical analysis presented above, numerical optimization was performed in order to obtain the optimal composition of the CBPC formulated with LG-MgO. The basic concept of optimization means a compromise in some values in order to reach higher values in others. The properties with respect to which this optimization was performed were chosen as maximal compressive strength at 7 and 28 days, assuming that mechanical properties at 1 day

Table 7
Optimization target for factors and responses and suggested formulations.

Name	Goal	Upper limit	Lower limit	F1	F2	F3
LG	In range	55	65	62.5	61.9	58.4
HB	In range	0	3	0.57	0.64	0.52
Setting time initial (min)	In range	20	30	20.00	21.02	20.00
Setting time final (min)	In range	25	45	42.19	45.00	45.00
CS 1 day (MPa)	In range	1.08	41.45	26.52	23.43	23.71
CS 7 days (MPa)	Maximize	20.13	41.28	39.15	39.21	36.99
CS 28 days (MPa)	Maximize	21.19	52.94	42.37	41.30	35.73

will evolve and an adequate range of setting times in order to guarantee an acceptable workability. The goal for each response is shown in Table 7; based on the mentioned criteria three optimum formulations suggested by the model, F1, F2 and F3 are shown in the same table.

3.3. CBPC. Structural characterization

A representative number of the specimens used in the compressive strength tests were examined after fracture using XRD and SEM, in order to provide information on microstructure.

The diffraction pattern of all CBPC specimens formulated with LG-MgO (e.g. Fig. 8) shows K-struvite –$KMgPO_4{\cdot}6H_2O$– as major crystalline phase, as well as magnesite, dolomite, quartz, calcite, anhydrite and periclase magnesium oxide. It should be noted that stable phases contained in the LG-MgO did not react and remain unchanged. The presence of arcanite –K_2SO_4– should also be noted, which is formed from the excess potassium that has not reacted during the formation of K-struvite. Likewise, one may also conclude that K-struvite was the sole magnesium phosphate formed, and no other crystalline phases as such bobierrite –$Mg_3(PO_4)_2{\cdot}8H_2O$– or newberyite –$MgHPO_4{\cdot}3H_2O$– were identified. However, no presence of lunebergite or any other boron-magnesium crystalline phase

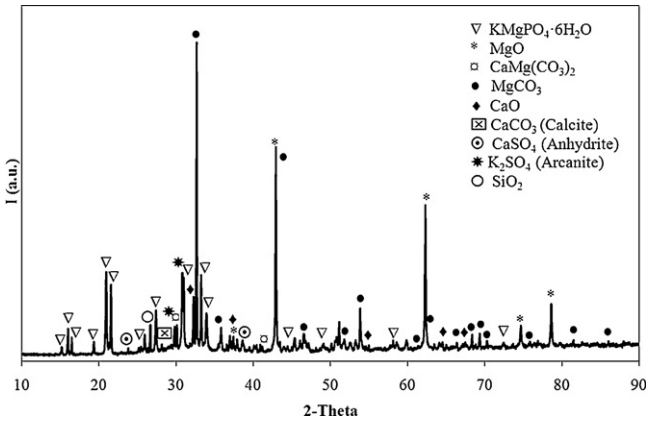

Fig. 8. X-ray pattern of CBPC formulated with LG-MgO. 60LG3H curing for 28 days.

was identified, unlike what has been described in the literature for similar HB/S ratios [9,11]. In this case, lunebergite can be dissolved before the setting age studied or be rendered totally X-ray amorphous.

Fig. 9 shows the SEM micrograph of the fractured surface of a CBPC formulated with LG-MgO (60LG) and carbon coated. The micrograph shows a material consisting of particles embedded in a K-struvite matrix. The fracture surface of the

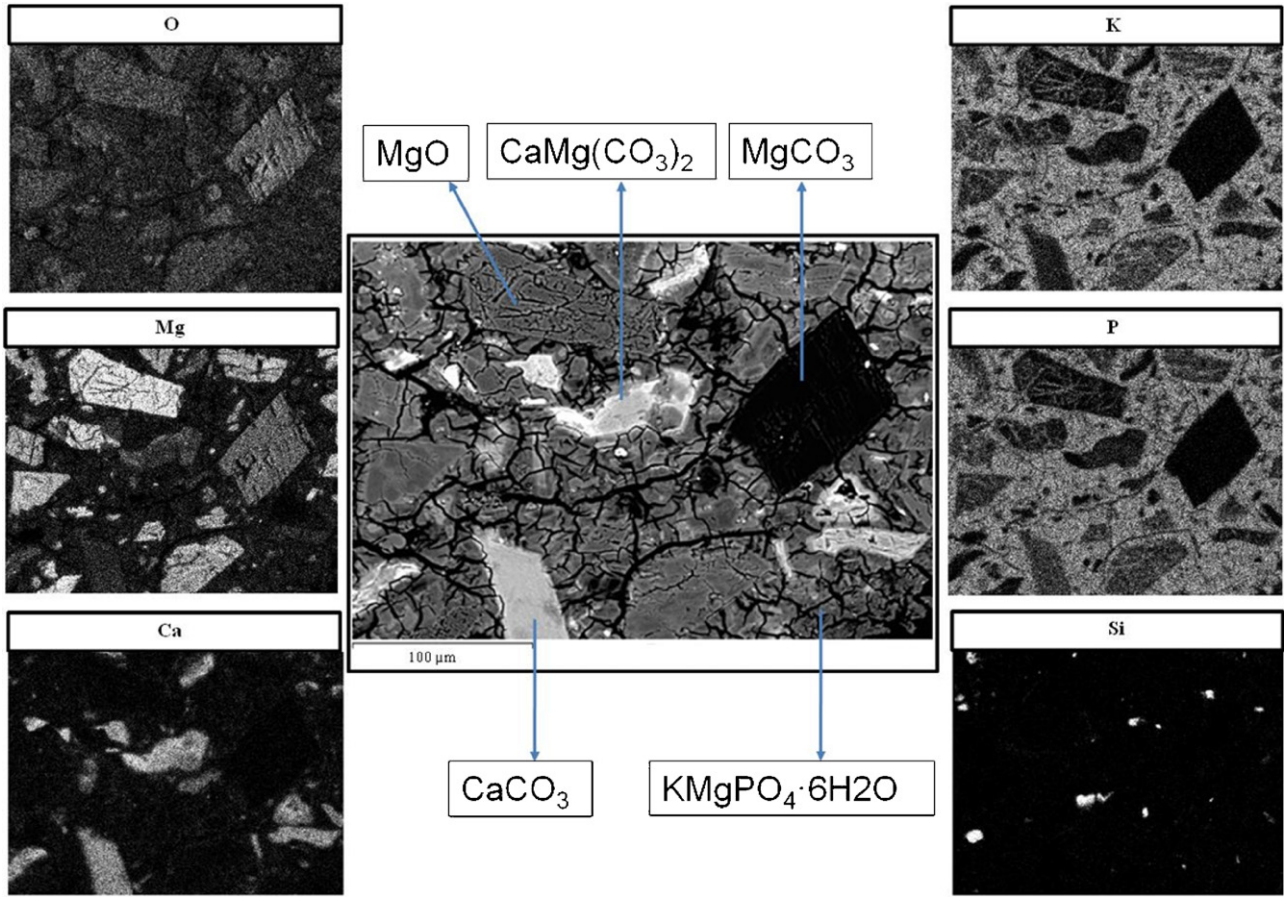

Fig. 9. SEM micrograph of fractured surface of a CBPC specimen formulated with LG-MgO (60LG). EDS X-ray maps of O, Mg, Ca, K, P and Si. 60LG cured for 28 days.

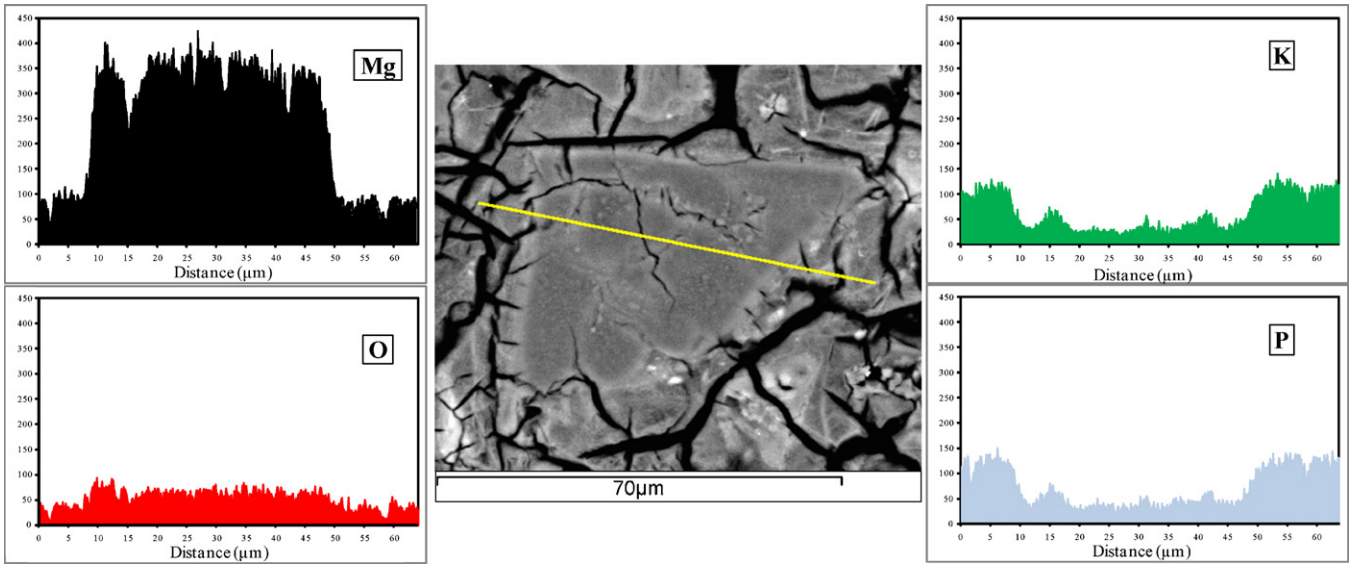

Fig. 10. EDS linescan of a particle of periclase embedded into K-struvite matrix. 60LG cured for 28 days.

binder phase is relatively dense and becomes rough, showing a high degree of microcraking, which indicates that higher levels of stress and strain occurred during fracture [26].

The semi-quantitative X-ray mappings in Fig. 9 show the elemental distribution and location of O, Mg, Ca, K, P and Si in the cement. These maps confirm the previous identification made by XRD. Thus, from the relative abundance of the elements and taking into account the crystalline phases determined by XRD, magnesite, dolomite, quartz and periclase particles were observed and located in the K-struvite matrix. When the reactivity and solubility of magnesia are very low and the particle is non-porous, the reaction begins on the outside of the particle and moves towards the centre, proceeding via a non-reacted core model. In this case, the unreacted nucleus remains unchanged and becomes a filler particle.

The angular and rough particles are randomly distributed in the matrix as a fine filler of the cement paste, thereby improving the compressive strength of the product. Moreover, on the contact surface between the unreacted nuclei of periclase and the K-struvite matrix, the phosphate ions diffuse into the surface forming a layer around the particles. Hence, the remaining particles of periclase, though an inert filler, improve the mechanical properties of the cement. This layer around the periclase particles creates a strong bond between the particles and cement matrix.

This fact can be observed in the EDS line scan across a periclase particle embedded into a K-struvite matrix of a CBPC formulated with LG-MgO (Fig. 10). This scan semi-quantitatively shows the relative intensities of the different elements across the particle and the nearby matrix. Thus, the line scan drawn on the micrograph is initiated in the binder matrix, then crosses the MgO particle and finally ends again in the matrix that covers the opposite side of the particle. As can be observed in Fig. 10, the level of magnesium is uniformly high throughout the entire particle of periclase and the interface region, whereas the level decreases sharply when the scanning line meets the K-struvite matrix. The relative intensity of magnesium in the binder matrix is related with potassium and phosphorus, implying the same abundance in the cement according to the molar ratio in the K-struvite. Moreover, the relative intensity of potassium inside the periclase particle coincides with the phosphorus intensity, being both very low, which can only be attributed to background noise or interference.

4. Conclusions

It is feasible to formulate CBPC using magnesium by-products collected in the gas cleaning systems of the natural magnesite calcination process. LG-MgO has the appropriate particle size and reactivity for a correct formulation, without the need to proceed to a subsequent calcination to reduce its reactivity. Hence, the use of LG-MgO reduces the cost of the final product and increases the competitiveness of the magnesium CBPC, while reinforcing criteria of sustainability and recyclability.

In the formulation of phosphate cements, as a result of the low MgO content in the by-product and the low reactivity of the same, a larger amount of LG-MgO than those formulated with pure MgO is required. Furthermore, the presence of non-reacting phases in the LG-MgO and the unreacted nuclei of MgO strongly bonded to the K-struvite matrix both enable inorganic fillers to be included, thereby improving the mechanical properties of cement. Furthermore, as described in the literature, the use of boric acid as a setting retardant also improves the workability of pastes.

The statistical method was employed to predict the effects of variables on final properties. It was established a model which explains the overall behaviour of the system which could not be studied using a single variable method. This set of models allows not only to estimate the response of each formulation but also to optimize the whole system to obtain a compromise between the factors constraints and the responses obtained.

According to the setting times and compressive strength results, the formulations 60LG0.5H to 1.0H may be chosen as a satisfying range to be used, for example, for cement repair. These formulations comprise the addition of 60% of LG-MgO and 40% of MKP, as well as an amount between 0.5% and 1.0% of boric acid as setting retardant, with water to solid ratio about 0.24. It is expected that all of them will show good workability and applicability for cement repair. In addition, this CBPC series shows good mechanical properties from the first curing day, the compressive strength in this period being greater than that described in the literature for cements formulated with pure MgO, with values greater than 40 MPa, which remain constant from the 7th curing day.

Acknowledgements

The authors would like to thank Magnesitas Navarras S.A., the Spanish Ministry of Science and Innovation (Project FIS2009-13360-C03-03) and the Generalitat of Catalonia (Project 2009SGR878) for supporting and financing this research project.

References

[1] D.M. Roy, New strong cement materials: chemically bonded ceramics, Science 235 (1987) 651–658.
[2] A.S. Wagh, R. Strain, S.Y. Jeong, D. Reed, T. Krause, D. Singh, Stabilization of rocky flats Pu-contaminated ash within chemically bonded phosphate ceramics, J. Nucl. Mater. 265 (1999) 295–307.
[3] I. Buj, J. Torras, D. Casellas, M. Rovira, J. de Pablo, Effect of heavy metals and water content on the strength of magnesium phosphate cements, J. Hazard. Mater. 170 (2009) 345–350.
[4] I. Buj, J. Torras, D. Casellas, M. Rovira, J. de Pablo, Leaching behaviour of magnesium phosphate cements containing high quantities of heavy metals, J. Hazard. Mater. 175 (2010) 789–794.
[5] P. Randall, S. Chattopadhyay, Advances in encapsulation technologies for the management of mercury-contaminated hazardous wastes, J. Hazard. Mater. B114 (2004) 211–223.
[6] A.I. Borzunov, S.V. D'yakov, P.P. Poluéktov, Immobilization of radioactive wastes by embedding in phosphate ceramic, Atom. Energy 96 (2004) 123–126.
[7] Q. Yang, B. Zhu, S. Zhang, X. Wu, Properties and applications of magnesia-phosphate cement mortar for rapid repair of concrete, Cem. Concr. Res. 30 (2000) 1807–1813.
[8] F. Qiao, C.K. Chau, Z. Li, Property evaluation of magnesium phosphate cement mortar as patch repair material, Constr. Build. Mater. 24 (2010) 695–700.
[9] A.S. Wagh, S.Y. Jeong, Chemically bonded phosphate ceramics: a dissolution model of formation, J. Am. Ceram. Soc. 86 (2003) 1838–1844.
[10] S.Y. Jeong, A.S. Wagh, Chemically Bonded Phosphate Ceramics: Cementing the Gap between Ceramics and Cements, Argonne National Laboratory, 2002.
[11] A.S. Wagh, Chemically Bonded Phosphate Ceramics Twenty-First Century Materials with Diverse Applications, first ed., Elsevier B.V., Amsterdam, 2004.
[12] M.A. Carvalho, A.M. Segadães, The hydration of magnesium phosphate cements: effect of powder characteristics on the reaction kinetics, Mater. Sci. Forum 591–593 (2008) 833–838.
[13] A.K. Sarkar, Phosphate cement-based fast-setting binders, Am. Ceram. Soc. Bull. 69 (1990) 234–238.
[14] P.K. Sen Gupta, G.H. Swihart, R. Dimitrijevic, M.B. Hossain, The crystal structure of lunebergite, $Mg_3(H_2O)_6[B_2(OH)_6(PO_4)_2]$, Am. Mineral. 76 (1991) 1400–1407.
[15] J.M. Chimenos, A.I. Fernandez, G. Villalba, M. Segarra, A. Urruticoechea, B. Artaza, F. Espiell, Removal of ammonium and phosphates from wastewater resulting from the process of cochineal extraction using MgO-containing by-product, Water Res. 37 (2003) 1601–1607.
[16] J.M. Chimenos, A.I. Fernandez, A. Hernandez, L. Haurie, F. Espiell, C. Ayora, Optimization of phosphate removal in anodizing aluminium wastewater, Water Res. 40 (2006) 137–143.
[17] J. Formosa, M.A. Aranda, J.M. Chimenos, J.R. Rosell, A.I. Fernández, O. Ginés, Chemically bonded cements formulated with by-products of magnesium oxide, Bol. Soc. Esp. Ceram. Vidr. 47 (2008) 293–297 (in Spanish).
[18] R.R. Menezes, H.G. Malzac Neto, L.N.L. Santana, H.L. Lira, H.S. Ferreira, G.A. Neves, Optimization of wastes content in ceramic tiles using statistical design of mixture experiments, J. Eur. Ceram. Soc. 28 (2008) 3027–3039.
[19] N. Schlechtriemen, J.R. Binder, R. Knitter, J. Haußelt, Optimization of feedstock properties for reaction-bonded net-shape zircon ceramics by design of experiments, Ceram. Int. 36 (2010) 223–229.
[20] D.C. Montgomery, Design and Analysis of Experiments, third ed., John Wiley & Sons, New York, 1991.
[21] M. Niubó, A.I. Fernández, L. Haurie, X.G. Capdevila, J.M. Chimenos, J.I. Velasco, Mater. Sci. Eng. A 528 (2011) 4437–4444.
[22] M.A. Shand, The Chemistry and Technology of Magnesia, John Wiley & Sons Inc. Publication, New Jersey, 2006.
[23] C.A. Strydom, E.M. Van der Merwe, M.E. Aphane, The effect of calcining conditions on the rehydration of dead burnt magnesium oxide using magnesium acetate as a hydrating agent, J. Therm. Anal. Calorim. 80 (2005) 659–662.
[24] D.A. Hall, R. Stevens, B. El-Jazairi, The effect of water content on the structure and properties of magnesia-phosphate cement (MPC) mortar, J. Am. Ceram. Soc. 81 (1998) 1550–1556.
[25] J. Formosa, J.M. Chimenos, A.M. Lacasta, L. Haurie, Thermal study of low-grade magnesium hydroxide used as fire retardant and in passive fire protection, Thermochim. Acta 515 (2011) 43–50.
[26] D.A. Hall, R. Stevens, B. El-Jazairi, The effect of retarders on the microstructure and mechanical properties of magnesia-phosphate cement mortar, Cem. Concr. Res. 31 (2001) 455–465.